Met. Mater. Int., Vol. 16, No. 5 (2010), pp. 755~760
doi: 10.1007/s12540-010-1009-4 Published 26 October 2010

Electro-Deposition Behaviors of Trivalent Chromium during Pulse Plating

Yong Choi*

Department of Advanced Materials Engineering, Sunmoon University,
100 Galsan-ri,Tangjeoung-myeon, Asan-si, Chungnam 336-840, Korea

(received date: 19 February 2010 / accepted date: 2 May 2010)

Thick trivalent chromium layers were prepared in a modified chromium sulfate bath by pulse plating to replace hexavalent hard chromium coating in industrial fields; layer microstructure development was systematically studied by using electron microscopy and small angle neutron scattering (SANS) to give a model for nucleation and growth behaviors during the pulse plating. Finer columnar grain was formed by pulse plating due to its high nucleation rate at the same current density. Average deposition rate of the trivalent chromium layers is in the range of 32.4 μm/h to 49.7 μm/h. The deposition rate increases as the diameter of cylindrical shape of chromium cluster in a columnar grain is reduced. The highest deposition rate in this study was observed under the conditions of direct current density of 0.4 Acm^{-2}, combined with a rectangular shape pulse current density of 1.5 Acm^{-2} with a 10/2 on-off time ratio. Most of the inner-cracks of the trivalent chromium layers have dimensions in the range of about 39 nm. Ultrasonic agitation during pulse plating resulted in an increase of neutral salt fog spray life, which is related to smaller crack size and broader size distribution in the trivalent chromium.

Keywords: thin film, deposition, microstructure, neutron scattering, pluse plating

1. INTRODUCTION

Eco-friendly trivalent chromium has been attracting attention because of its environmental safety [1]. Although technology to make thin and decorative trivalent chromium layers has been used in some applications like ornaments and emblems, electrochemical methods to deposit relatively thick trivalent chromium that can replace the hexavalent hard chromium used in the automobile and electronic industries are still under development [2,3].

One of the problems in making industrially applicable thick trivalent chromium layers is the low neutral salt fog spray life, which is due to the poor microstructure, including inner-cracks, formed by hydrogen evolution during electroplating [4].

Microstructure development during electro-deposition includes nucleation and growth processes. This kind of electro-deposition process can be classified into five steps: ion migration, reduction, surface migration and diffusion, growth, and, finally, hydrogen gas evolution [5,6]. Since the double layers in front of the electrode and the ion migration to the electrode play important roles during the electro-deposition process, columnar grains containing metallic clusters are usually formed under an electro-chemical potential. The competitive behavior of the deposition and the hydrogen gas evolution result in the introduction of inner cracks [7,8]. It means that a high quality trivalent chromium layer can be obtained by preventing the abnormal growth of columnar grains and by removing hydrogen gas effectively during electroplating. There have been many studies on methods to control the microstructure by changing current wave form and solution chemistry. Among these methods, pulse plating, in which the pulse current changes the double layers in front of the electrode, has been found attractive because it makes a so called “crack free” chromium surface [9]. However, previous techniques that have been used to observe the microstructure of the chromium layer have not been able to give sufficient information about actual inner-cracks and the microstructure of the electrodeposited layers because of destructive sample preparation methods and local observation area [10,11].

Accordingly, reliable methods to analyze the microstructure of chromium and the inner cracks should be chosen in order to study the nucleation and growth mechanisms during electro-deposition and to find the optimum plating conditions for use in industrial fields.

Hence, the objectives of this study are to investigate the nucleation and growth behaviors of thick trivalent chromium layers formed by pulse plating with ultrasonic agitation and

*Corresponding author: yochoi@sunmoon.ac.kr

to quantitatively analyze the nano-sized cracks in the chromium layer by using small angle neutron scattering for the production of high quality trivalent chromium in industrial fields.

2. EXPERIMENTAL METHOD

Electro-plating was carried out in a Hull cell containing a modified chromium sulfate bath. Table 1 shows the solution chemistry of the modified chromium sulfate bath. The anode and the cathode were a titanium electrode and an AISI 1040 steel plate, respectively. Ultrasonic agitation at 500 W was applied to the electro-deposition cell with an ultrasonic generator (Daejin-BH-50, Korea) during electro-deposition. The electroplating was carried out with a regulator (Jisan-400, Korea) with different current wave forms such as a direct current density of 0.4 Acm^{-2}, a rectangular shaped pulse current density of 1.5 Acm^{-2} with different on-off time ratio, and ultrasonic agitation.

A neutral salt fog spray test (Cotec-NSF, Korea) was performed to evaluate the chromium quality. Microstructure was observed by field emission scanning electron microscopy (Jeol JSM-6700F, Japan). Surface roughness was determined by atomic force microscopy (Parks Instrument, USA). Small angle neutron scattering (SANS) was carried out to analyze the nano-sized inner-cracks of the trivalent chromium layers (HANARO, Korea Atomic Energy Research Institute, Institute of Metal Physics, Russia Academy of Science, Russia). Raw data were analyzed by using the SASFIT program [12].

Table 1. Solution chemistry of a modified chromium sulfate bath (wt.%)

$Cr_2(SO_4)_3{\cdot}nH_2O$	HCOOH	K_2SO_4	$(NH_4)_2SO_4$	H_3BO_3	NH_4Br
44.3	14.6	6.3	6.3	25.3	3.2

3. RESULTS AND DISCUSSION

3.1. Nucleation

Figure 1 shows the surface morphology of the eco-friendly trivalent chromium layers as observed by scanning electron microscopy. As shown in Fig. 1, fine grain size on the surface was observed in the pulse plated chromium for similar thickness of about 30 μm. In order to quantitatively analyze the surface morphology, surface roughness was determined by atomic force microscopy. Figure 2 shows the surface roughness and topography of the chromium layers as observed by atomic force microscopy for the 1000 nm of the scanning range on the surface. As shown in Fig. 2, the average surface roughness is 19.5 nm for the pulse plated chromium layer and 54.3 nm for the direct plated chromium layer. These results support the idea that the grain size of pulse plated chromium is finer than that of direct current plated chromium.

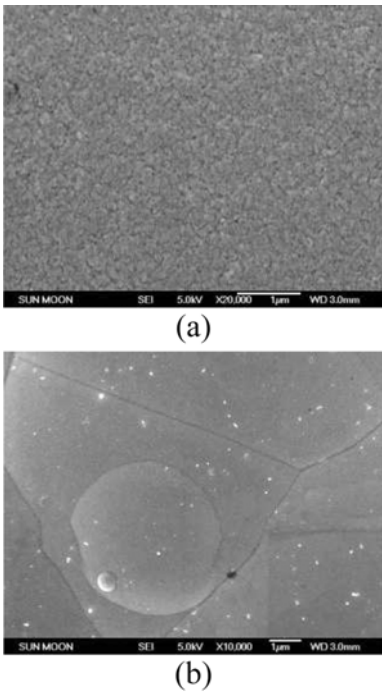

Fig. 1. Surface morphologies of the chrome layers for a given plating time of 2.5 hour at different plating condition : (a) msec-pulse plating (t_{on}/t_{off} = 10/0.5) (b) direct plating.

The reason why grain size is reduced by pulse plating can be explained by classical nucleation theory, in which fine grains are related to high nucleation rate. The nucleation rate under the conditions of electroplating is described by the following equation [13]:

$$J = k_1 \exp(-k_2/\eta_2)$$

where k_1 and k_2 are constants and η_2 is the over potential. For the activation controlled electro-deposition process, the equation can be simplified into the following equation, based on the Bulter-Volmer equation [14]:

$$\eta = \eta_{o_c} \ln \frac{i}{i_o}$$

where η_{o_c} and i_o are the cathodic Tafel slope and the exchange current density, respectively. Since the average current density (i_{av}) of the pulse plating is normalized by the on and off time ratio ($t_{off}/t_{on} = p > 0$), such as $iav = i_c/(1+p)$, the over potential (η_A) at the electrode for the same current density is always greater during pulse plating than it is during direct current plating.

$$\eta_A = \eta_{0c} \ln \frac{i}{i_0} = \eta_{0c} \ln \frac{i_{av}(1+p)}{i_0}$$

$$\eta_A(pulse) = \eta_A(D.C)$$

These results show that pulse plating always gives a higher

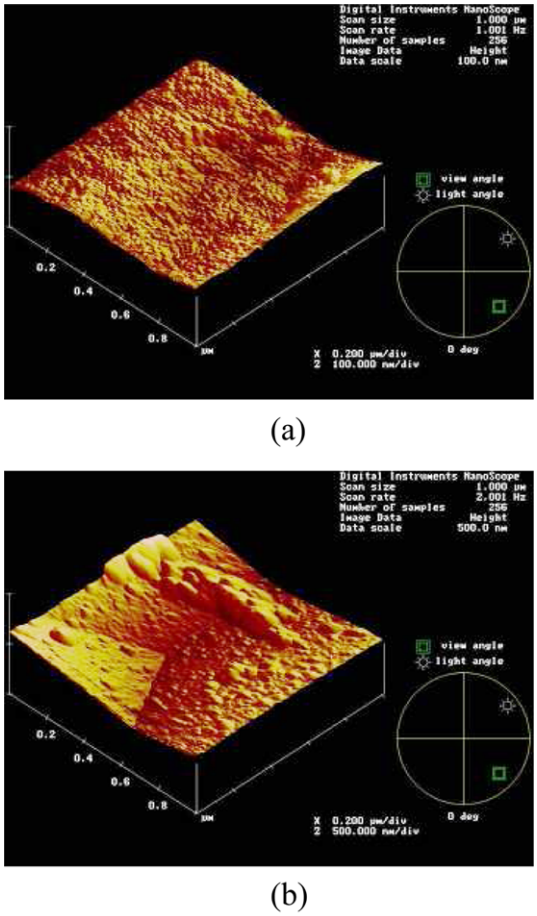

Fig. 2. Surface roughness and topography of the chrome layers for a given plating time of 2.5 hour at different plating condition : (a) msec-pulse plating (t_{on}/t_{off} = 10/0.5) (b) direct plating.

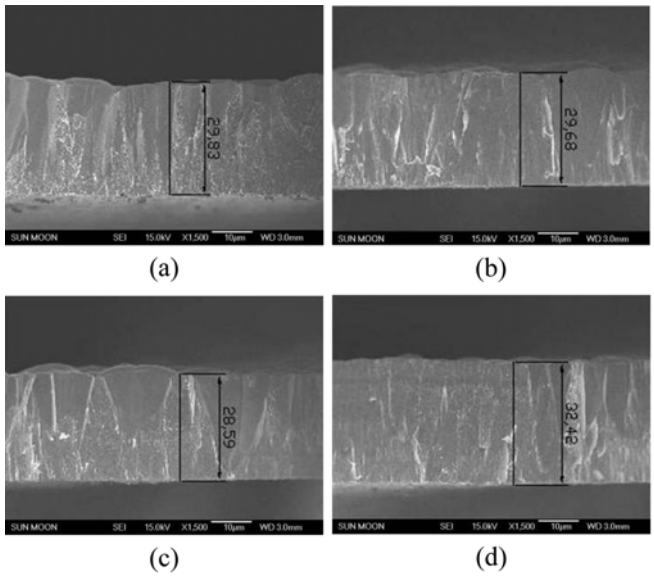

Fig. 3. Chromium thickness change prepared at the direct current density of 0.4 Acm^{-2} with a rectangular shape pulse current density of 1.5 Acm^{-2} with different on-off time ratio at the same potential of 4.8 V: (a) t_{on}/t_{off} = 10/0.2 (b) 10/0.5 (c) 10/0.7 (d) direct current only.

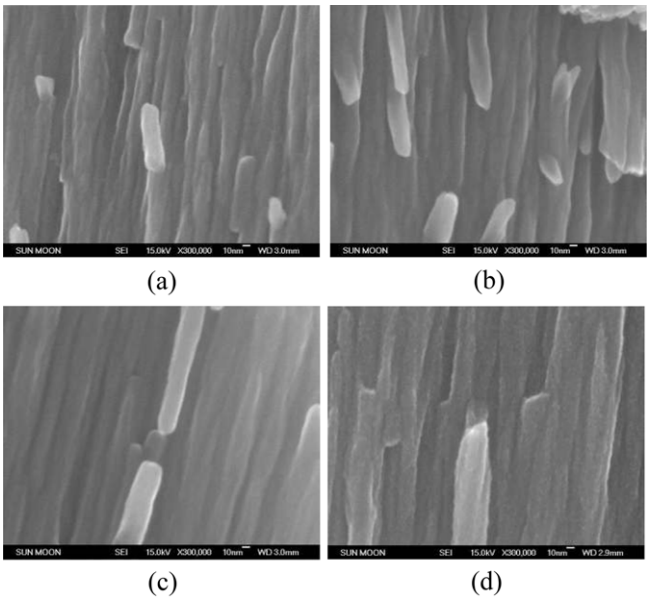

Fig. 4. High magnification of chromium clusters in columnar grains prepared at the direct current density of 0.4 Acm^{-2} with a rectangular shape pulse current density of 1.5 Acm^{-2} with different on-off time ratio at the same potential of 4.8 V: (a) t_{on}/t_{off} = 10/0.2 (b) 10/0.5 (c) 10/0.7 (d) direct current only.

nucleation rate at the same current density, resulting in the formation of finer grains.

3.2. Growth

Although the microstructure of electro-deposited chromium includes metallic chromium and inner-cracks, macroscopic growth rate is related to chromium thickness for an effective given plating time. Figure 3 is a cross-sectional view of the chromium layers with different current wave forms. As shown in Fig. 3, the trivalent chrome layers with equal current density but different pulse on and off time ratio give different chromium thickness.

Considering the electro-deposition process, the growth behavior of chromium grain can be described by a monolayer model of chromium clusters because the chromium grain consists of chromium clusters that are formed layer-by-layer. Since a columnar grain of the chromium contains a chromium cluster, the cluster size is related to the growth rate. In order to find a cluster size with plating conditions, a cross-section of the chromium layer was observed by field emission electron microscopy. Figure 4 gives an image with high magnification of the columnar grain of the chromium layer, in which chromium clusters with cylindrical shape were well observed. The diameter of the cylindrical chromium cluster changes with electro-plating conditions. Table 2 summarizes the chromium thickness and the diameter of the cylindrical chromium cluster with the plating conditions. The average deposition rate is in the range of 32.4 μm/h to

Table 2. Thickness of chromium layer, plating time, growth rate and diameter of chromium cluster with plating condition

on/off [msec]	thick [μm]	On Time [min]	Eff. [μm/min]	Cluster Dia. [nm]
P10/0.2	29.83	36	0.829	20-25
P10/0.5	29.68	45	0.660	22-26
P10/0.7	28.59	51	0.561	25-27
DC only	32.42	60	0.540	30-35

49.7 μm/h.; the highest deposition rate in this study was observed at the direct current density of 0.4 A cm^{-2} with a rectangular shape pulse current density of 1.5 Acm^{-2} and with a micro-second 10/0.2 on-off time ratio. Interpreting the data shown in Figs. 3 and 4, and in Table 2, it is clear that the smaller diameter of the cylindrical cluster shape gives a higher growth rate for the pulse plating.

This kind of cluster growth behavior can be expressed by using a classical monolayer growth model combined with cluster size [15,16]. The rate of lateral growth (V) of a cluster is expressed with monolayer step (d) of a cluster and atomic diameter (n), and vibration frequency (ν) of ad-atom on a cluster surface; the geometrical direction for the atomic jumping on a cluster surface is determined by the following equation :

$$V = \frac{\nu d}{6}\left\{\exp\left(-\frac{\Delta\eta}{KT}\right) - \exp\left(-\frac{\Delta(\eta+\eta_A)}{KT}\right)\right\}$$

For small over-potential change under activation control, Δη, (ex|x→0≈1), the rate of lateral growth (V) of a cluster, becomes the following equation:

$$V = \frac{\nu d}{6} \cdot \frac{\eta_A}{KT}$$

Since the number of monolayers on a cluster is proportional to the height of columnar grains, the time to reach to the end of a cluster edge becomes shorter as the cluster diameter becomes smaller for the same over-potential. Accordingly, the vertical growth velocity (H) of a columnar grain becomes faster when the cluster diameter is small at the same potential. This is in good agreement with the microstructure observation shown in Fig. 4.

3.3. Inner cracks

Since electro-deposited chromium consists of metallic chromium and inner-cracks, actual deposition rate should consider both chromium growth rate and number of inner cracks. Inner cracks in the electro-deposited chromium layers are inevitably formed in the electroplated chromium due to hydrogen evolution and abnormal growth of columnar grains. Since the crack size and distribution is a barometer indicating the electro-deposited chromium quality, crack size can be indirectly evaluated by a neutral salt fog spray test in industrial field.

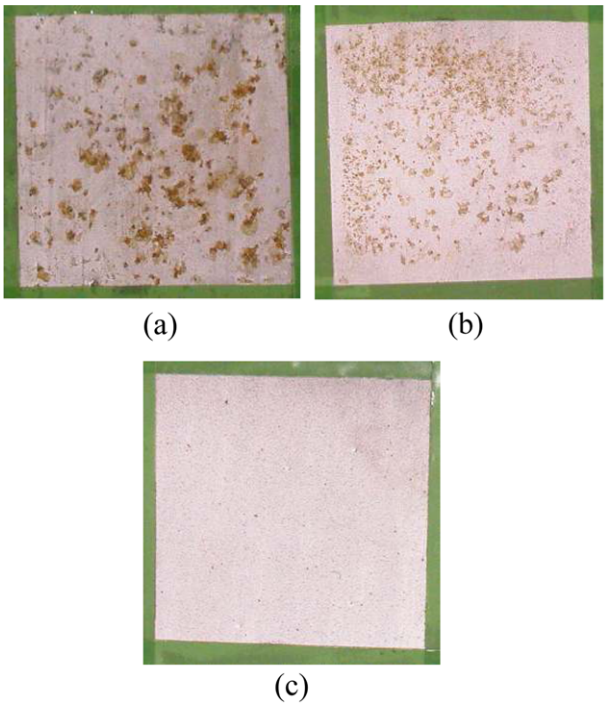

Fig. 5. Chromium surface after 72 hours neutral salt fog spray test : (a) direct current density of 0.4 Acm^{-2}, (b) a rectangular shape pulse current density of 1.5 Acm^{-2} with 1 msec on-off time ratio (c) a rectangular shape pulse current density of 1.5 Acm^{-2} with 1 msec on-off time ratio with ultrasonic agitation.

Figure 5 is chromium surface after 72 hours of neutral salt fog spray test on the trivalent chrome layers formed by various plating conditions, such as only direct current density of 0.4 Acm^{-2}, pulse density with pulse peak voltage of 4.8 V, and pulse plating with ultrasonic agitation. As shown in the Fig. 5, the chromium layer prepared by ultrasonic pulse plating shows better neutral salt fog spray life than the chromium layer prepared without ultrasonic agitation. Since the neutral salt fog spray test is related to crack size and to the distribution of the chromium layers, small angle neutron scattering was applied to determine the crack size and distribution in this study to keep from introducing artificial cracks during sample preparation and to quantitatively evaluate the cracks.

Figure 6 is the typical small angle neutron scattering (SANS) spectra of the trivalent chrome layers formed by various plating conditions in which a neutron beam penetrates the chromium layer perpendicularly. As shown in Fig. 6, an intensity peak of SANS spectra was clearly observed at the Q value of 0.16. Since the intensity of SANS describes the lattice or the ordered arrangement of repeated motifs, the peak position is used to estimate the ordered structure in a range of 1 nm to 100 nm [17]. By using the equation such as $Q^* = 2\pi/D$ based on Bragg's law, the Q value of the peak

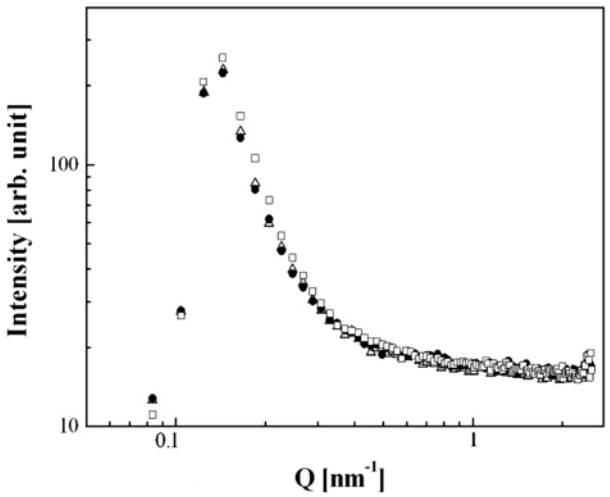

Fig. 6. Distribution of nano-size cracks in electroplated chromium layers with plating conditions : direct current density of 0.4 Acm^{-2} (□), a rectangular shape pulse current density of 1.5 Acm^{-2} with 1 msec on-off time ratio without (△) and with ultrasonic agitation (●).

intensity with 0.16 is estimated to be about 39 nm of the repeated motifs [18]. It is interesting what the repeated motifs to give the SANS spectra are. Considering the microstructure of the chromium layers as seen in Fig. 4, and the results of neutral salt fog spray test of the chromium layers as seen in Fig. 5, the chromium layers consist of two physically separated phases like metallic chromium and inner cracks. Chromium as a major phase of the layer contributes the SANS spectra in all scattering ranges with similar intensity values, whereas, because of their position and distribution in the chromium layer, cracks as minor phases of the layer make intensity peaks in a local scattering range with different intensity values. This means that the repeated motifs that make the intensity peaks are related to the inner cracks in the chromium layer. Accordingly, the intensity as absolute cross section and momentum transfer scattering vector (Q) of the SANS spectra, as seen in Fig. 6, are related to the relative number and size of inner cracks. In other words, most of the cracks in the trivalent chromium layers prepared by direct current plating, whether pulse plating and ultrasonic pulse plating are, in the range of about 39 nm. The number of cracks in the chromium layer, which is proportional to the intensity, is the lowest in the ultrasonic pulse plated layer, that is lower than those in the other chromium layers formed by direct current and pulse plating without ultrasonic agitation. Although it is difficult to precisely determine actual crack size because the cracks exist as isolated or inter-connected types, it is clear that relatively smaller cracks exist in the chromium layer prepared by ultrasonic pulse plating. This supports the idea that the high neutral salt fog spray test life of the chromium layer prepared by pulse plating with ultrasonic agitation is related to the smaller number of inner cracks.

The next interesting point is why ultrasonic pulse plating produces smaller inner crack sizes in the trivalent chromium layers. The answer can be obtained by considering the electro-deposition mechanism [6,7,19]. The ultrasonic agitation influences the microstructure development of the trivalent chromium layer during the electro-deposition process. The electro-deposition process includes five steps: ion migration, reduction, surface migration and diffusion, growth, and hydrogen gas evolution. Hydrogen ions besides metallic ions are reduced during the charge-transfer reaction and the hydrogen gas evolution occurs on the substrate surface. Since the hydrogen gases on the substrate cause interference with the ad-atom deposit behavior, these gases make fine cracks, whether in the grain or at the grain boundary. Since ultrasonic agitation enhances the reduction of concentration polarization in front of the cathode and the effective removing of hydrogen gas embryo on the cathode, a few defects have a chance of existing and interconnecting in the chromium layer. Hence, the chromium layers prepared by pulse with ultrasonic agitation method have smaller and more isolated cracks, which results in a better neutral salt fog spray life.

4. CONCLUSIONS

Eco-friendly trivalent chromium layers were prepared in a sulfate bath; layer electro-deposition behaviors were studied to obtain information about microstructure development during the electro-plating for use in industrial fields. The results are summarized as follows:

1. Average surface roughness of the trivalent chromium layers with similar thickness of about 30 μm is 19.5 nm for pulse plated layers and 54.3 nm for direct plated layers. Pulse plating results in finer grain size on the surface than conventional direct current plating does, because of the former method's high nucleation rate at the same current density.

2. Average deposition rate of the trivalent chromium layers prepared in this study is in the range of 32.4 μm/h to 49.7 μm/h. The highest deposition rate was observed under the conditions of direct current density of 0.4 Acm^{-2} combined with a rectangular shape pulse current density of 1.5 Acm^{-2} with 10/2 on-off time ratio. Chromium growth rate with columnar grain becomes faster as the chromium cluster diameter becomes smaller.

3. Most of the cracks in the trivalent chromium layers prepared for this study have dimensions in the range of about 39 nm, whether they are interconnected or not. Ultrasonic agitation during the pulse plating process resulted in improved neutral salt fog spray life of the chromium layers because this agitation reduces inner crack size and broadens crack size distribution.

ACKNOWLEDGMENTS

This work was supported by a Korea Research Foundation Grant funded by the Korean Government (KRF-2009-013-D00003-100645). The author would like to thank Dr. S. C. Kwon and Dr. M. Kim of KIMS, Dr. E. J. Shin and Dr. B. S. Seong of KAERI, professor J. K. Lee of Michigan Technological University, professor A. Pirogov of IMP in Russia, and professor M. Sarikaya of the University of Washington for the initiation of this study and valuable discussion.

REFERENCES

1. M. S. Chandrasekar and M. Pushpavanam, *Electrochem. Acta* **53**, 3313 (2008).
2. I. Drela, J. Szynkarczuk, and J. Kubicki, *J. Appl. Electrochem.* **19**, 933 (1989).
3. H. H. Wan and H. Y. Cheh, *J. Electrochem. Soc.* **135**, 643 (1988).
4. J. S. Kim, R. H. Song, S. I. Pyun, and H. C. Kim, *J. Mater. Sci*. **24**, 2704 (1989).
5. Y. Choi, *J. Mater. Sci. Lett.* **15**, 629 (1996).
6. N. V. Mandich, *Plat. Surf. Finish.* **84**, 108 (1997).
7. Y. Choi, *J. Mater. Sci.* **32**, 1581 (1997).
8. Y. Choi, M. Kim, and S. C. Kwon, *Surf. Coat. Tech.* **169**, 81 (2003).
9. J. C. Puippe, *Theory and Practice of Pulse Plating*, p. 177, American Electroplaters Society (1986).
10. Y. Choi, M. Y. Choi, Y. S. Hahn, M. Kim, and S. C. Kwon, *Mater. Sci. Forum.* **475**, 4005 (2005).
11. S. G. Pyo, D. W. Lee, and S. B. Kim, *Met. Mater. Int.* **14**, 773 (2008).
12. K. Kohlbrecher, *SASFIT (c), version 08.2*, PSI, Switzerland (2007).
13. P. Leisner, G. Bech-Nielsen, and P. Møller, *J. Appl. Electrochem.* **23**, 1232 (1993).
14. O. M. Bockris, A. K. N. Reddy, and M. Gamboa-Aldeco, *Modern Electrochemistry 2A. Fundamentals of Electrodics, 2nd ed.*, p. 1083, Kluwer Academic/Plenum Publishers (2000).
15. M. Jalochowski, M. Hoffmann, and E. Bauer, *Phys. Rev. Lett*. **51**, 7231 (1995).
16. C. M. Pina, D. Bosbach, M. Prieto, and A. Putnis, *J. Cryst. Growth* **187**, 119 (1998).
17. R.-J. Roe, *Method of X-ray and Neutron Scattering in Polymer Science*, p. 15, Oxford University Press, New York (2000).
18. N. Laversanne, *J. Phys. Chem. B* **105**, 11081 (2001).
19. Y. Choi, *J. Kor. Inst. Met. & Mater.* **34**, 773 (1996).